A Diagnostic Study of the Wind- and Buoyancy-Driven North Atlantic Circulation

MICHAEL A. SPALL

Woods Hole Oceanographic Institution, Woods Hole, Massachusetts

A two-moving-layer diagnostic model with a variable depth mixed layer on top is applied to the annual mean climatology of the North Atlantic. Estimates of the annual mean mass flux from the mixed layer into the upper thermocline (called mixed layer pumping) and subsurface heating rates are obtained on the basin scale from hydrographic data alone. No independent measures of wind stress or other surface forcings are required. In addition, it is shown that the nonlinear terms in the vorticity equation are critical to balance the subsurface heat flux in the Gulf Stream and over most of the subtropical gyre. Evidence is presented for the existence of interior, southeastern, northeastern, and recirculation regimes in the North Atlantic. These regimes are distinguished by the behavior of the characteristic trajectories of the system and by whether the flow is a direct cell (interfacial flux and vertical velocity have the same sign) or indirect cell (interfacial flux and vertical velocity have the opposite sign). It is demonstrated here that one can make use of analytic approaches in the analysis of historical data sets to yield relatively simple solutions that give a direct link between theory and observations.

1. INTRODUCTION

The present analysis takes a diagnostic approach to study the influences of combined wind and buoyancy forcing in the North Atlantic basin. The model is similar to the two-moving-layer model of *Luyten and Stommel* [1986] (hereafter LS) but with more general forcing, including a variable depth mixed layer. Instead of imposing the interfacial fluxes and solving for the layer depths, as in many previous analytic models, we assume the layer depths are known from climatological hydrography and solve the system of equations for the interfacial mass fluxes consistent with the model dynamics. These interfacial fluxes represent the annual mass flux through the base of the mixed layer and the subsurface heating rate. We interpret the solution in terms of the role of the nonlinear Jacobians and, by making use of the quasi-linear form of the equations, the nature of the characteristics of the system.

It is generally believed that both wind and buoyancy forcing are important to the general circulation in the North Atlantic, although influences of these combined effects are difficult to observe directly. Analytic studies by *Luyten and Stommel* [1986] and *Pedlosky* [1986] have helped to identify some basic consequences of including buoyancy forcing in an idealized basin. These models impose simple forms for the Ekman pumping, subsurface interfacial heating, and boundary conditions and then solve for the depths of the layer interfaces in an idealized basin. Each method, however, relies heavily on this assumed knowledge of the interface forcing and boundary conditions. *Cushman-Roisin* [1987a] presents a similar two-layer, analytic, quasi-geostrophic model of the subtropical gyre-recirculation system in which the Ekman pumping is specified but the interfacial heating is determined by a relaxation of the interface depth to some equilibrium value. Primitive equation general circulation models allow for more general forcing and interbasin exchange, but

their solutions are often quite complicated and their interpretation is much less straightforward than that for the analytic models. In an interesting diagnostic study by *Luyten et al.* [1985] the nonlinear geostrophic layer equations are used to study the effects of buoyancy forcing in the North Atlantic Current. However, this type of model also has an assumed knowledge of the surface forcing, and its results can be quite sensitive to the choice of model parameters and region, making its application on the basin scale uncertain.

The paper is outlined as follows. The model and characteristic equations are presented in section 2. A diagnostic calculation of the North Atlantic circulation is carried out in section 3. The results are discussed in section 4, and final conclusions are presented in section 5.

2. THE LAYER EQUATIONS

We assume the ocean is made up of four layers with the deepest layer at rest, as shown in Figure 1. The uppermost layer (layer 0) represents the mixed layer, while the middle two layers (layers 1 and 2) represent the upper thermocline, assumed to be geostrophic and hydrostatic on the beta plane. Layers 1, 2, and 3 are each assumed to be of uniform density. Let η, h and D be the depths of the mixed layer, the first interface, and the second interface, respectively. We may then write the equations for mass conservation in the geostrophic layers 1 and 2 as

$$- \gamma_1 J(h, \eta) + \gamma_2 J(D, h - \eta) - \frac{\beta}{f}(h - \eta)(\gamma_2 D + \gamma_1 h)_x$$
$$= \frac{f}{g}(w_i - w_{ml}) \quad (1)$$

and

$$\gamma_2 J(h, D) - \frac{\gamma_2 \beta}{f}(D - h)D_x = -\frac{f}{g}w_i. \quad (2)$$

The Jacobian operator is defined as $J(a, b) = a_x b_y - a_y b_x$ and $\gamma_n = 10^3(\rho_{n+1} - \rho_n)/\rho_0$. The left-hand side of each equation is made up of nonlinear Jacobian and beta terms. The Jacobian in equation (2) represents the net mass flux across the interface between layers 1 and 2 as a result of the
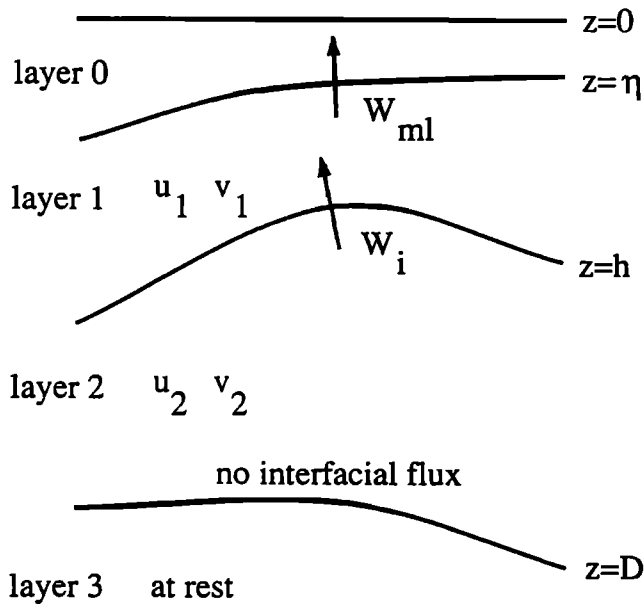
Fig. 1. Schematic of model layers: layer 0 is the mixed layer, layers 1 and 2 represent the upper thermocline, and layer 3 represents the deep ocean, assumed to be at rest.

horizontal advection through the sloping interface h. The two Jacobian terms in equation (1) represent the flux into layer 1 through the upper and lower interfaces by the horizontal advection through the sloping interfaces at $z = \eta$ and $z = h$. The right-hand sides represent the net flux of mass into each layer across the upper and lower interfaces. The flux from the mixed layer into layer 1, w_{ml}, may be attributed to the vertical Ekman pumping velocity, the horizontal shoaling of the mixed layer, and the time rate of change of the local mixed layer depth [*Cushman-Roisin*, 1987b].

$$w_{ml} = w_e + \vec{v} \cdot \nabla \eta + \eta_t \qquad (3)$$

Because of the fundamental role both Ekman pumping and the mixed layer play in determining w_{ml}, we will refer to this mass flux from the mixed layer into layer 1 as the mixed layer pumping. The sign convention is chosen such that a mass flux from the upper thermocline into the mixed layer is positive.

The flux through the interface at depth h is w_i; a positive value represents a flux from layer 2 into layer 1. Such a conversion of heavier water into lighter water would also imply that there is some heating taking place. (In the following discussion we will refer to changes in density as heating or cooling processes, although the same effects could be accomplished by changes in salinity. There is no way to distinguish between thermal and saline effects in the present model.) It is therefore through the cross-interfacial flux term $J(h, D)$ that the buoyancy driving enters the system. This interfacial flux is, of course, an oversimplification of the actual physical process which takes place in the ocean. It is, however, consistent with the present large-scale, steady, discrete model, and it seems reasonable to represent these unresolved processes in terms of their net influence on the mass balance. Wind forcing enters through the familiar relationship between the wind stress curl and the vertical velocity at the surface of layer 0, the Ekman pumping contribution to the mass flux. It is important to note that, as a result of the nonlinear Jacobian terms, the net mass flux between each

of the layers does not need to be vertical. We assume there is no mass flux through the interface at $z = D$.

Equations (1) and (2) may be solved for the interfacial fluxes w_{ml} and w_i. We note here that there is no need for an independent estimate of the surface forcing, such as the assumed Ekman pumping used in previous analytic models, to calculate the mass fluxes and subsurface heating rate.

Equations (1) and (2) have been derived from mass continuity, but they may also be written in the form of a potential vorticity equation. From this perspective, the interfacial flux works to increase or decrease the layer thickness and thus contributes to the local potential vorticity balance. The diagnostic approach used here calculates the left-hand side of equations (1) and (2) and interprets the residual in terms of the interfacial fluxes. In the model of *Rhines and Young* [1982], the right-hand side of the potential vorticity equation is attributed to eddy fluxes of potential vorticity, written as $K = \nabla(\kappa \nabla q)$, where κ is the eddy diffusivity and q is the potential vorticity. The ratio of the buoyancy forcing to the eddy flux in the potential vorticity equation (α) is

$$\alpha = \frac{fLd^2 \delta w}{\kappa U H} \qquad (4)$$

where U, L, H, d are typical values of the horizontal velocity, horizontal length scale, layer thickness, and deformation radius, f is the Coriolis parameter, and δw is the net interfacial flux into the layer. Thus, as the interfacial fluxes go to zero (appropriate for the deep ocean, as in the study of Rhines and Young), the eddy flux becomes dominant, while for vanishing eddy diffusivity the diabatic processes are dominant. This expression may be further simplified if we assume that the interfacial flux divergence is the same order of magnitude as the vertical gradient in the Ekman pumping velocity, $\delta w/H = \beta U/f$. The ratio is now written as

$$\alpha = \frac{Ld^2 \beta}{\kappa} \qquad (5)$$

This result is similar to that obtained by *Pedlosky* [1983], who used an integral approach to compare the influences of eddy mixing and ventilation following a parcel circulating throughout the subtropical gyre. Taking values typical of the mid-latitude subtropical gyre, $L = 1000$ km, $d = 50$ km, $\beta = 10^{-11}$ m^{-1} s^{-1}, and $\kappa = 10^3$ m^2 s^{-1}, the ratio of diabatic processes to eddy fluxes is found to be 25. Thus, for the large-scale flow in the upper thermocline of the subtropical gyre, the residual of the nonlinear potential vorticity equation may be reasonably interpreted as diabatic processes represented by the interfacial fluxes w_i and w_{ml}.

The interfacial fluxes are calculated as the residual of a nonlinear equation and, as such, may be strongly dependent on the values used for the interface depths. The errors introduced into the interfacial fluxes are linearly proportional to errors in the layer thicknesses and nonlinearly proportional to errors in the slopes of the layer interfaces. A 10% error in the layer thickness will result in only a 10% error in the interfacial flux. However, the net contribution from the Jacobian terms is actually due to the difference between two larger terms. For the present calculation, a 10% error in the interface slope will result in approximately a 30% error in the interfacial flux. Although the resulting errors could be fairly large, this degree of sensitivity is acceptable for the present study because the primary objectives here are to investigate processes and qualitative behavior, not to make

a quantitative estimate of the actual heating and cooling rates.

We now derive the characteristic form of equation (2). An advantage of this form is that, for a given interfacial flux w_i and the Ekman pumping w_e, one may solve for the layer depths h and D using the method of characteristics, as shown by LS. In the present diagnostic study, we do not need to resort to the method of characteristics to solve for the interfacial depths because we assume these are known from climatological hydrographic data. We include the characteristic form here, however, because the nature of the characteristic trajectories is used to identify different dynamical regimes within the flow and is also helpful in giving insight into the interpretation of the interfacial velocities and interface depths. Equations (1) and (2) are first added to give

$$J(\eta, \gamma_2 D + \gamma_1 h) + \frac{\beta}{f}\eta(\gamma_1 h + \gamma_2 D)_x -$$

$$\frac{\beta}{f}(\gamma_1 h h_x + \gamma_2 D D_x) = -\frac{f}{g}w_{ml} \qquad (6)$$

The Jacobian represents the advection through the mixed layer interface by the layer 1 geostrophic velocity. Making use of equation (3), and assuming that the annual contribution from the local change in mixed layer depth (η_t) is zero, equation (6) can be rewritten as

$$\gamma_1(h - \eta)h_x + \gamma_2(D - \eta)D_x = \frac{w_e f^2}{\beta g}. \qquad (7)$$

If we also assume that $\eta \ll h, D$ (later shown to be true), then equation (7) may be integrated in x to give

$$\frac{1}{2}(\gamma_1 h^2 + \gamma_2 D^2) = \int_{x_0}^{x} \frac{w_e(x,y)f^2}{\beta g} + C(y) = G(x,y). \qquad (8)$$

This relation is similar to that derived by LS, where w_e was assumed to be a function of latitude only. Here we leave the right-hand side as a general function of x and y. The derivatives of h are now eliminated from equation (2) to give

$$\left[-\frac{g\gamma_2 G_y}{\gamma_1 f D} - \frac{\gamma_2 \beta g h}{f^2 D}(D - h)\right]D_x + \frac{g\gamma_2 G_x}{\gamma_1 f D}D_y = -\frac{h}{D}w_i. \qquad (9)$$

Equations (8) and (9) constitute the quasi-linear form of the governing equations. Written in terms of the characteristic velocities (v_c and u_c), equation (9) becomes

$$u_c D_x + v_c D_y = -\frac{h}{D}w_i = D_\zeta. \qquad (10)$$

The meridional characteristic velocity (v_c) is equivalent to the average geostrophic meridional transport over the two moving geostrophic layers. This is driven by the mixed layer pumping and the Sverdrup balance. The zonal characteristic velocity (u_c) is made up of two terms: the first is the averaged geostrophic transport, and the second is the westward nondispersive propagation speed of a Rossby wave confined to the upper ocean. The change in depth of the second layer along the characteristic trajectory (D_ζ) is driven by the interfacial flux w_i.

3. THE DIAGNOSTIC CALCULATION

The layer equations from section 2 are now applied to the annual mean hydrographic data of *Levitus* [1982]. The values of h and D are taken from the climatology at 1° resolution, and the zonal and meridional derivatives are calculated

using centered differences. The region under study extends from 10°N to 55°N and from 65°W to 20°W. The model domain is indicated in Figure 2, superimposed on the estimated vertical velocity at the base of the Ekman layer [from *Leetmaa and Bunker*, 1978]. An attempt has been made to apply the model to the ocean interior, where the geostrophic approximation is most valid. The domain does extend close to the coastline in two regions: Newfoundland enters the domain in the northwest corner, and South America enters the domain in the southwest corner. These two regions have been masked out of the diagnostic calculations.
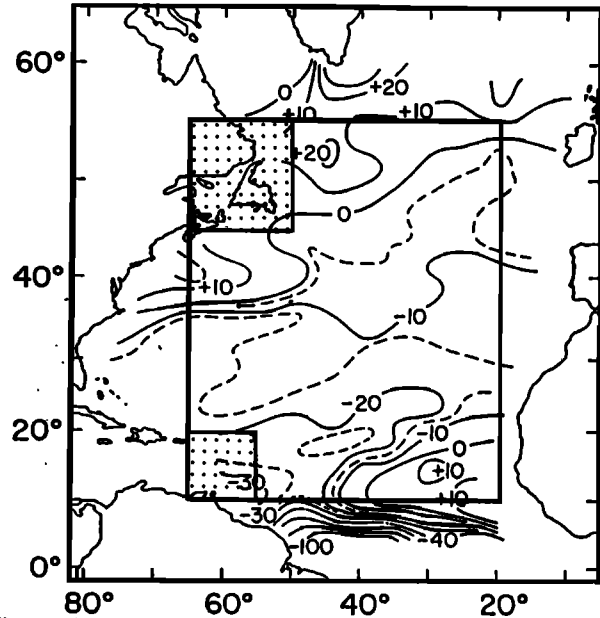

Fig. 2. Annual mean vertical velocity at the base of the Ekman layer, 10^{-5} cm s^{-1} [from *Leetmaa and Bunker*, 1978].

Interface 1 is defined by the depth of the potential density surface $\sigma_0 = 26.5$; interface 2 is defined by density surface $\sigma_0 = 26.7$, where $\rho = \rho_0(1 + 10^{-3}\sigma_0)$. The density at the base of the mixed layer is taken to be 26.1, representative of the annual mean at the mid-latitudes of the subtropical gyre. The densities of layers 1 and 2 are then calculated as $\rho_1 = (26.1+26.5)/2$ and $\rho_2 = (26.5+26.7)/2$. The density of the deepest layer is assumed to be $\rho_3 = 27.4$ (approximately 800 m in the subtropical gyre), so that $\gamma_1 = 0.3$ and $\gamma_2 = 0.8$. The mixed layer depth (η) was calculated from the annual mean density field using the $\Delta\sigma = 0.125$ criterion. The solution is not calculated where $h < \eta$, near the outcrop of the upper layer.

There are, of course, many ways to decompose the continuous density profile into a discrete system, particularly when the model is being applied over an area containing many dynamical regimes. Since a primary interest of the present study is the role of the nonlinear Jacobian terms, we have chosen our two geostrophic layers to best represent the beta spiral over most of the subtropical gyre. Of course, other layers could be chosen, and they will give results which are qualitatively similar but which will be different in the details.

It is assumed that the density is constant within each geostrophic layer. This is a good approximation for layer 2 because it is bounded by surfaces of constant density. However, in the real ocean, layer 1 would have a decreasing av-

erage density as one moved further to the south because the density of the mixed layer decreases to the south. It is impossible to include these effects in a two-moving-layer model, but this is noted as a possibly important limitation of the simplification.

One must also be cautious about the interpretation of the results in the Gulf Stream region. The climatological data are strongly smoothed there, due to both the temporal variability of the stream and the analysis method of *Levitus* [1982]. In addition, the Gulf Stream is approximately geostrophic in only one direction; this model neglects the relative vorticity (which is large in the synoptic Gulf Stream) and assumes that the deepest layer is at rest, while it is known that the Gulf Stream has velocity signatures deep

into the water column. Furthermore, eddy fluxes of potential vorticity may also be contributing to the right-hand sides in equations (1) and (2), while the residuals are presently interpreted as interfacial fluxes only. However, it is believed that the qualitative results of the present model are representative of the large-scale dynamics in this region, but that the quantitative aspects must be interpreted with these approximations in mind.

Figures 3a–3d plot h, D, $h + D$, and G. The depth of interface 1 is approximately 200 m to 300 m, and the depth of interface 2 is approximately 300 m to 500 m over most of the subtropical gyre. The direction of flow in the second layer is along lines of constant D, while the direction of flow in the upper layer is along lines of constant $h + D$.
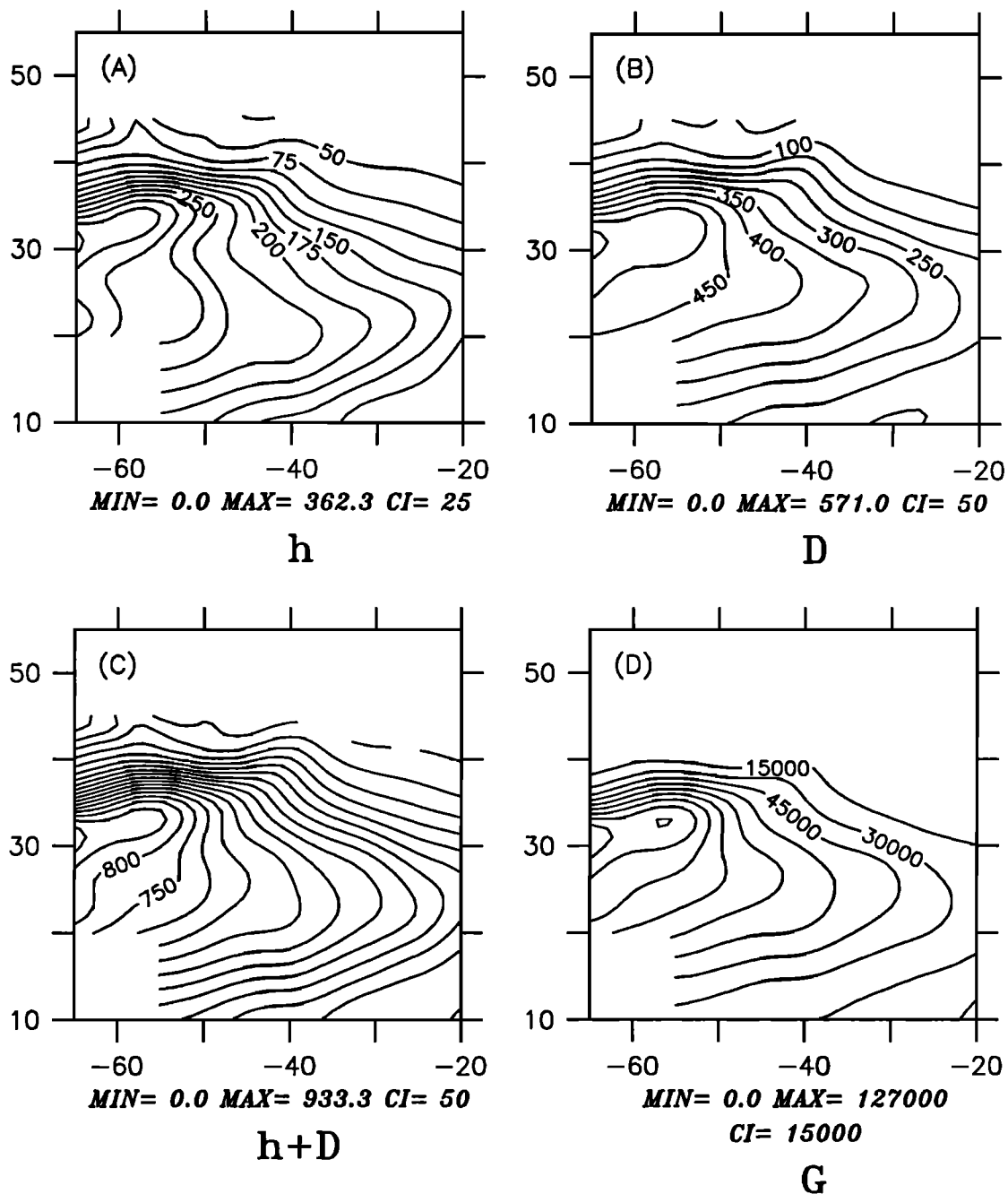

Fig. 3. (a) Depth of the first layer, h. (b) Sum of layers 1 and 2, $h + D$. (c) Depth of the second layer, D. (d) Forcing function G.

Several well-known features of the subtropical gyre are evident from the interface depths. The strong sloping density surfaces in the northwest mark the Gulf Stream region; it enters near 35°N and flows toward the northeast. The gyre recirculation is indicated in both the upper and lower layers as the flow turns to the southeast, peeling away from the Gulf Stream. A rotation of the velocity vector with depth is implied in Figures 3b and 3c by the nonparallel trajectories, consistent with the expected beta spiral in that region. It is under such conditions that we expect the nonlinear terms in equations (1) and (2) to be important.

The forcing function G is calculated directly from the interfacial layer depths as $\frac{1}{2}(\gamma_1 h^2 + \gamma_2 D^2)$. G appears similar to the form used by LS, which was derived from an Ekman

pumping velocity which was sinusoidal in latitude, but the present forcing contains more structure, particularly in the western portion of the domain. The Gulf Stream is characterized by strong meridional gradients in G, while the maximum to the south of the Gulf Stream is consistent with the local increase in the Ekman pumping (see equation (8)) implied by climatological wind stress data in Figure 2. We see later that this local maximum influences the propagation of characteristic trajectories in this region.

The annual mean mixed layer depth is shown in Figure 4. It is fairly shallow over most of the region of interest, so our approximation $\eta \ll h, D$ used to derive the characteristic equation is valid. The mixed layer is deepest in the far northeastern region, near 55°N, and in the eastern subtropical gyre, near 20° to 25°N. Over most of the subtropical gyre interior the mixed layer depth is nearly uniform between 20 m and 30 m depth.

We know that the depth of the mixed layer varies greatly over the annual cycle. In particular, during the winter months the mixed layer becomes very deep in the northern Atlantic, while during the summer it is quite shallow there. This winter deepening is believed to be important for the subduction of near-surface water into the thermocline. This effect is not explicitly represented in our present, steady model. The mixed layer pumping determined here is different from what is traditionally interpreted as the annual subduction rate. Subduction generally refers only to the mass flux from the mixed layer into the upper thermocline. In calculating an annual subduction rate, one usually does not consider the period when the flow is from the upper thermocline into the mixed layer. Mixed layer pumping is a measure of the annual mean mass flux from the upper thermocline into the mixed layer and takes into account both the subduction of water into and the removal of water from the upper thermocline.

The mixed layer pumping is calculated from equations (1) and (2) and shown in Figure 5a. This is the annual mean flux from the mixed layer into layer 1 which is required to maintain a mass balance in this discrete model. It is negative
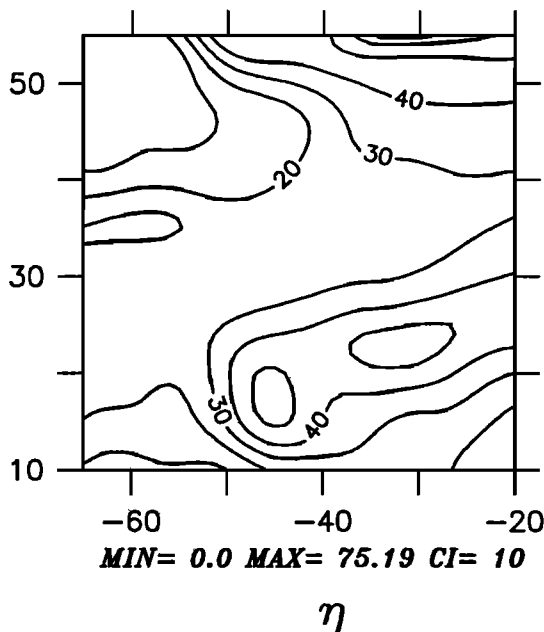

MIN= 0.0 MAX= 75.19 CI= 10

η

Fig. 4. Depth of the annual mean mixed layer based on $\Delta\sigma = 0.125$.

MIN=-46.16 MAX= 38.38 CI= 8

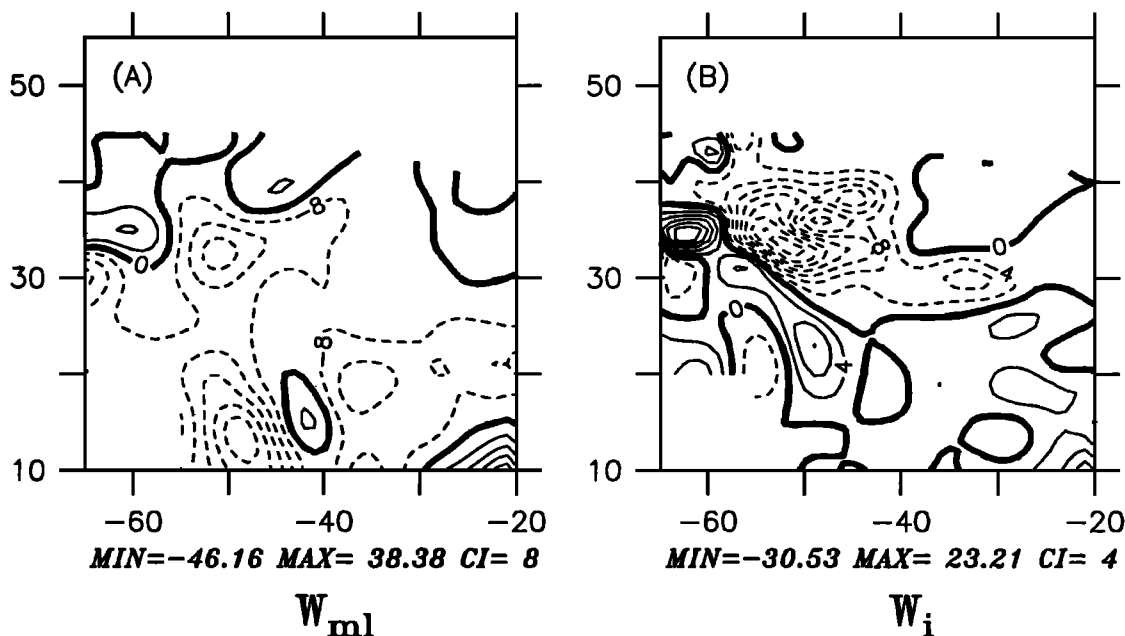W_{ml}

MIN=-30.53 MAX= 23.21 CI= 4

W_i

Fig. 5. (a) Mixed layer pumping, w_{ml}, and (b) interfacial velocity, w_i, in centimeters per day.

over most of the subtropical gyre, indicating a flow of water from the mixed layer into the upper thermocline. In the northeastern portion of the gyre the annual flux is small, less than 8 cm d^{-1}. Further to the south it increases and, to the west at about 50°W, becomes quite large. To the north, near 30°N, there are two local maxima just to the south of the Gulf Stream, at 65°W and 50°W. Along the northern side of the stream and in the southeast corner of the domain the mixed layer pumping is positive, consistent with the Ekman suction found in those regions (Figure 2). A more detailed analysis of mixed layer pumping and the relative contributions due to the Ekman pumping and shoaling of the mixed layer are given in section 4.

The interfacial flux (w_i) is shown in Figure 5b. It is obtained directly from equation (2) using the depths h and D. Over most of the low-latitude interior of the subtropical gyre the flux is slightly positive, on the order of 4 cm d^{-1}. This indicates that there is a weak heating taking place between the second and first layers, on the order of 4 W m^{-2}. The Gulf Stream is a region of negative flux as large as -30 cm d^{-1}, representing a heat loss of 30 W m^{-2}. The strong heat loss extends well south of the Gulf Stream into the northern portion of the recirculation region. There is also a much weaker negative interfacial flux throughout a broad northern region in the eastern basin at 30°N. The interfacial flux tends toward zero at the lowest latitudes, except in the southeast corner, where it is strongly positive.

We can also solve for the characteristic velocities in equation (9). The meridional characteristic velocity (Figure 6a) is almost everywhere toward the equator. This is as expected because it is closely linked to the Ekman pumping (equations (8) and (9)). The northward characteristic velocities in the western Gulf Stream and in the southeast corner are driven by the reversal of Ekman pumping. The zonal component (Figure 6b) shows a much different pattern. The characteristics emerge from the western boundary in the Gulf Stream (30°N to 40°N). In the interior, the entire northern portion of the domain contains eastward directed characteristics; however, they are much slower here

than in the Gulf Stream. Just south of the Gulf Stream there is a local maximum in the westward characteristic velocity. Along the eastern edge of the domain, characteristics may only enter south of 25°N, where the zonal characteristic velocity is negative. This change of sign along the eastern boundary is consistent with the analytical models of LS and *Pedlosky* [1986]; it indicates a transition from the western regime to the eastern regime. The portion of the eastern basin which is not accessible to characteristics which enter from the western regime is the shadow zone in the ventilated thermocline theory of *Luyten et al.* [1983]. Within the shadow zone, some of the characteristic velocities are directed to the northeast.

4. Discussion

The inverse approach taken here has allowed us to calculate the mass which must flow from the mixed layer into layer 1 over the annual cycle on the basin scale (w_{ml}) from hydrographic data alone. The actual processes which have gone into generating the climatology used here are strongly dependent on the annual cycle. Unfortunately, we cannot obtain direct estimates of the relative contributions due to the Ekman pumping and shoaling of the mixed layer, nor can we estimate the annual rate of water which is effectively subducted into the thermocline. The mass flux calculated here represents the net integrated effect of these complicated Lagrangian processes over the annual cycle. We do demonstrate here, however, that the present results are consistent with what would be expected based on the annual mean Ekman velocity, depth of the mixed layer, and equation (3).

In the eastern basin north of 25°N the mixed layer pumping is nearly zero (Figure 5a) while the Ekman velocity is fairly large, approximately -10 to -15 cm d^{-1} (Figure 2). This is explained by considering the annual mean of the terms in equation (3). It is known that the mixed layer slopes strongly downward to the north in this region during the winter. Such a slope would interact with the layer 1 flow (the flow direction is indicated in Figure 3c) to produce a net flux from the mixed layer into layer 1, a negative mixed
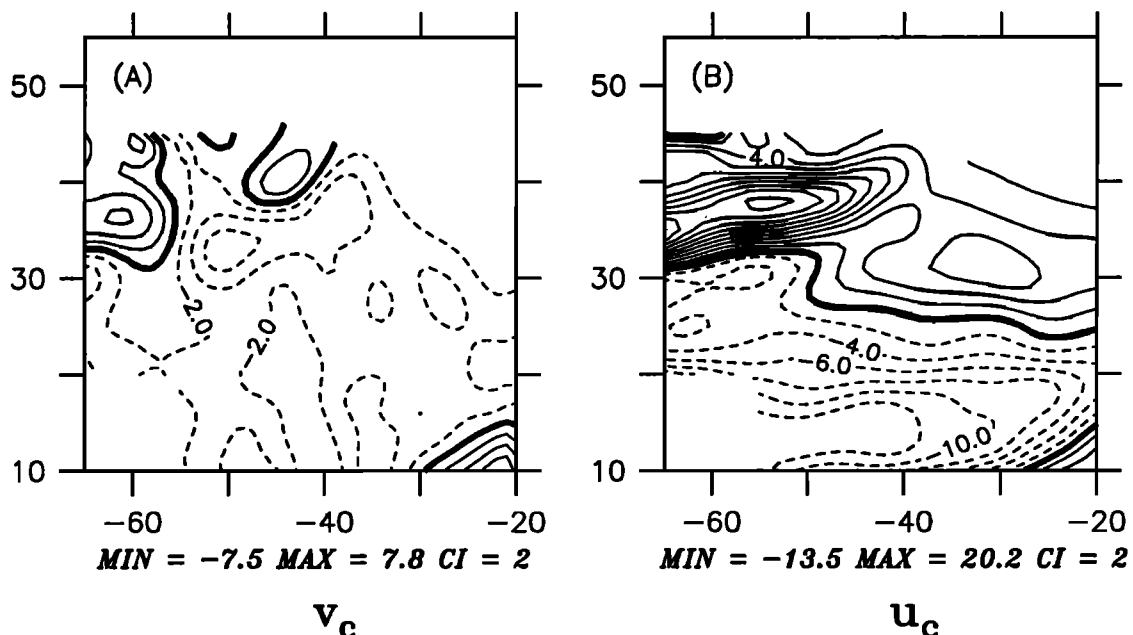

MIN = −7.5   MAX = 7.8   CI = 2   MIN = −13.5   MAX = 20.2   CI = 2

v_c u_c

Fig. 6. Characteristic velocities: (a) meridional velocity (v_c) and (b) zonal velocity (u_c).

layer pumping ($\vec{v} \cdot \nabla \eta < 0$). However, in the summer, the mixed layer slopes upward to the north, resulting in a positive contribution to the mixed layer pumping ($\vec{v} \cdot \nabla \eta > 0$). We can see from Figure 4 that over the annual mean the mixed layer slopes upward to the north with an amplitude as large as 4×10^{-5} m/m. The results presented here indicate that, over the annual mean, this net positive contribution is almost as large as the downward Ekman pumping ($\vec{v} \cdot \nabla \eta \approx -w_e$), resulting in nearly zero annual mixed layer pumping in the northeastern portion of the subtropical gyre. Further to the south (20°N), w_{ml} becomes more negative, approximately -16 cm d^{-1}. This change is driven by both a negative Ekman velocity and a reversal of the gradient of the mean mixed layer depth such that flow is from the mixed layer into layer 1. In the eastern shadow zone the mixed layer pumping is strongly positive, driven by both Ekman suction and the upper layer flow from a region with a shallow mixed layer depth into a region with a deeper mixed layer. To the west, south of 20°N, the flux becomes as large as -46 cm d^{-1}. This results from both an increase in the Ekman pumping (-30 cm d^{-1}) and a stronger gradient of the mixed layer depth. In this region, it is primarily the zonal flow which interacts with the mixed layer to produce the mixed layer pumping. To the north, just south of the Gulf Stream, the mixed layer is nearly uniform in depth and the Ekman pumping is the dominant forcing. The pattern of mixed layer pumping flux calculated here is consistent with the Ekman pumping seen in Figure 2. On the northern side of the Gulf Stream, the flux becomes positive, forced by a large Ekman suction which is slightly opposed by the advection of the mixed layer.

The subsurface heating rate (w_i) was also calculated using only the hydrographic data. The general pattern of weak heating over most of the mid-latitude subtropical gyre with strong heat loss in the Gulf Stream region is in qualitative agreement with the annual mean surface density flux calculated by Schmitt et al. [1989] using separate contributions from heat flux and evaporation minus precipitation. The amplitudes are reduced by roughly a factor of 5 at

this depth in the subtropical gyre (200 m to 300 m). The Gulf Stream is a region of strong cooling but, as a result of the model approximations, the quantitative value produced here may not be representative of the actual subsurface heat flux in this region. The warm water which is peeled off the Gulf Stream to feed the subtropical gyre recirculation is also cooled through the interfacial flux. This strong heat loss in the northern portion of the recirculation is also found at the surface in the data analysis of Isemer and Hasse [1987]. In addition, the analytic study by Cushman-Roisin [1987a] showed that cooling in this region was an important component of the basin scale potential vorticity budget. It is interesting to note that this cooling takes place where the meridional transport is toward the equator, not the pole.

The relative magnitudes of the terms in equation (2) are used to expose the roles of buoyancy and wind forcing in determining w_i. The purely vertical component of the interfacial flux arises as a result of the beta term (indirectly involving Ekman pumping) and is shown in Figure 7a. With the exception of a small region of upwelling in the western Gulf Stream and in the shadow zone, the vertical velocity at $z = h$ is negative throughout most of the subtropical gyre with maximum value at the mid-latitudes, as expected from the equatorward meridional transport and the downward Ekman pumping. The nonlinear Jacobian term (Figure 7b) is positive throughout the lower latitudes of the subtropical gyre, demonstrating that net positive interfacial flux is balanced by the nonlinear term which overcomes the negative vertical velocity. This nonvanishing sum of the two components of the Jacobian results from the clockwise rotation of the velocity vector with depth which is present throughout most of the subtropical gyre. In the northern portion of the gyre the warming results from the meridional component of the deep flow being directed from a region where the interface is shallow into a region where the interface is deep. In the southern portion of the gyre, the net positive flux is due to the zonal component of the deep flow being directed into a region where the upper layer is deepening. The sign of the interfacial flux in the subtropical gyre interior (Figure 5b)

MIN= -11.99 MAX= 17.13 CI= 4

$$-(D-h)\beta D_x/f$$
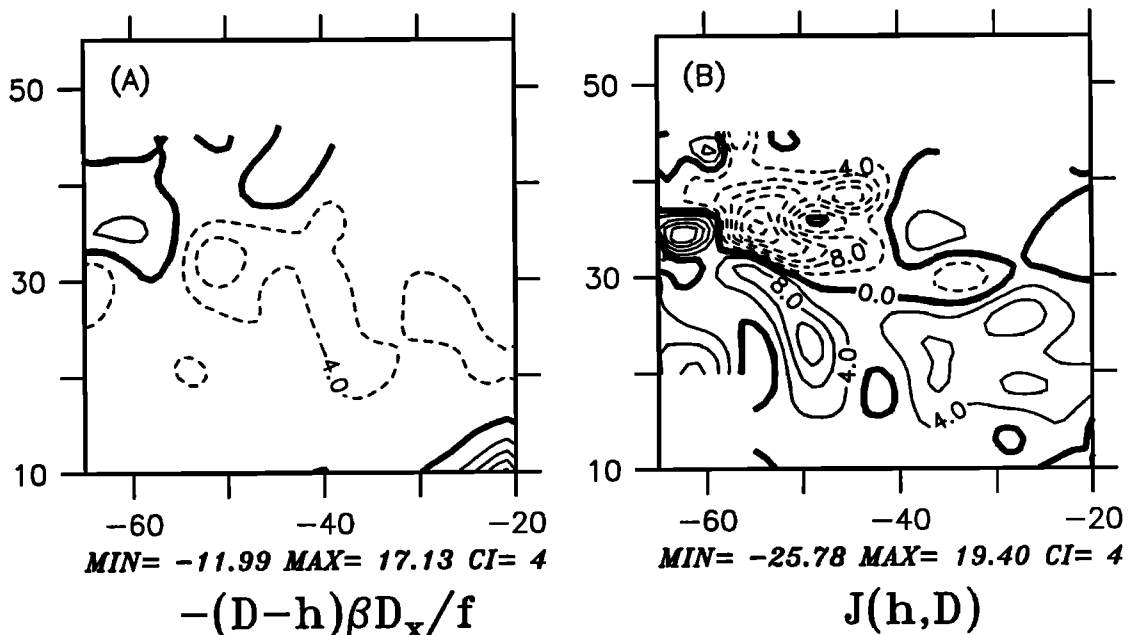
MIN= -25.78 MAX= 19.40 CI= 4

$$J(h,D)$$

Fig. 7. Terms in equation (3): (a) beta term and (b) Jacobian term.

is opposite to that of the vertical velocity (Figure 7a). This is the indirect cell which characterized the subtropical gyre interior in the analytic model of LS.

The indirect role of beta in balancing the upper ocean warming is really a very interesting and subtle one. Ekman pumping forces a negative vertical velocity in the upper ocean. The beta spiral, through this negative vertical velocity, causes the velocity vector to rotate clockwise with depth. This rotation brings into play the nonlinear Jacobian term which, through the horizontal advection of the interface depth, balances the conversion of the deep, dense water into the lighter upper ocean water. Therefore, throughout the subtropical gyre, there is a net mass flux into the lighter layer from the denser layer, even though the vertical velocity is negative. This situation stresses the importance of the nonlinear terms and emphasizes the fact that one must remember that the interfacial flux is not vertical.

We find here that there are large zonal variations in the interfacial flux and role of the nonlinear terms. In the western part of the basin at mid-latitudes the rotation of the velocity vector is increased, resulting in larger buoyancy forcing through the Jacobian term. In the eastern part of the gyre (at 30°N) the nonlinear contribution is found to be small, and the negative vertical velocity is balanced by βv, consistent with the beta triangle analysis of Armi and Stommel [1983]. The role of the nonlinear terms is also very small in the shadow zone region. It is interesting to note that the sign of the interfacial flux in the shadow zone is positive, the same sign as the Ekman pumping found there, and that the deep flow is directed to the northeast while the upper layer flow is directed to the southwest. This is the so-called direct cell predicted to exist in this region by LS and Pedlosky [1986]. A consequence of this positive interfacial flux is that, even with buoyancy forcing, the deep ocean in the eastern basin is not ventilated by water which was recently in contact with the upper ocean.

In the Gulf Stream and northern recirculation region, where the rotation of the velocity vector is counterclockwise with depth, the Jacobian dominates the beta term and balances a strong conversion of warm water to cold water. The transition of the clockwise spiral in the interior into the counterclockwise cooling spiral along the southern edge of the Gulf Stream is found in the numerical study of Spall [1991]. The interfacial flux and vertical velocity are both negative over most of the Gulf Stream, indicative of a direct cell in the terminology of LS.

Analyses of the characteristic trajectories indicate that the western and eastern regimes found in previous analytical models are also found here. The generality of the forcing in the present diagnostic model allows additional phenomena not permitted in the previous analytic studies, and thus motivates more specific names for each of the regions. In the present analysis, the western regime of LS is referred to as the interior regime, further distinguished by a Gulf Stream region, where information propagates in a narrow band very rapidly to the east, and a Sverdrup region, where the information propagates much more slowly and over a large range of latitudes. This Sverdrup region is analogous to the western regime of LS. A recirculation regime exists just south of the Gulf Stream, driven by the local maximum of the mixed layer pumping. Because the annual mixed layer advection is small here, this is closely related to the local maximum in Ekman pumping. This region is influenced by characteristics which originate in the Gulf Stream, turn to the south,

and then toward the west. The eastern regime of LS is called the southeastern regime here; it is indicated by a change in sign of the zonal characteristic velocity at about 25°N, originating at the coast of Africa. Those characteristics which originate along the eastern boundary within the southeastern regime define the shadow zone of Luyten et al. [1983].

The local magnitude of the characteristic velocity is shown in Figure 8. Two locations where both the zonal and meridional characteristic velocities are zero are indicated as R_c. Such points have been termed Rossby control points by LS because of the role of the westward Rossby wave propagation in determining their location. There is a Rossby control point in the shadow zone near 12°N, 20°W. This is analogous to one of the control points in the analytical model of LS. Characteristics originating from the south of this point are turned either to the west or toward the east, while characteristics from the northeast are deflected further to the west or turned sharply toward the coast. LS also found a control point in the northeast corner of the domain but, although the characteristics slow down there, we do not find one in the present model. Extending the analysis all the way to the coast in the northern region still does not result in a control point. This may be a consequence of the vertical discretization chosen for this study, which is intended to represent the gyre interior. As the thickness of layer 1 becomes small, the Rossby wave phase speed becomes small and less able to reverse the eastward advection of the subtropical gyre recirculation. A second control point is found, however, near the recirculation region in the western portion of the gyre, at 32° N, 60° W. The characteristic velocity goes to zero here because the depth-averaged flow vanishes at the center of the Gulf Stream recirculation. The westward Rossby wave propagation does not play a significant role in determining the existence of this control point, but its position is shifted slightly to the west as a result of the Rossby wave contribution. Nonetheless, characteristics cannot pass through this point, so in that sense it is worthy of mention.

$$MIN = 0.6 \quad MAX = 20.7 \quad CI = 2$$

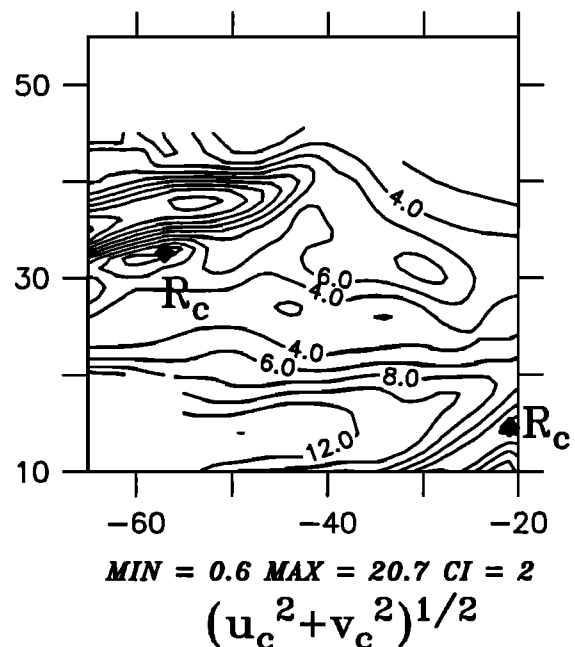$$\left(u_c^2 + v_c^2\right)^{1/2}$$

Fig. 8. Magnitude of the characteristic velocity $(u_c^2 + v_c^2)^{1/2}$.

It is interesting to note that the zonal characteristic velocity is almost as large in the southern part of the domain as it is in the Gulf Stream even though the advective speeds are much slower in the south. This is because the depth-averaged velocity and Rossby wave phase speed are additive in the south, while in the Gulf Stream region the Rossby wave propagation acts to oppose the eastward advective velocity.

The characteristic velocities in Figure 6 may be used to trace trajectories of the characteristics as they pass through the gyre. This is helpful to visualize paths along which information is transmitted as well as to indicate separate dynamical regimes within the basin. Four characteristic trajectories are shown in Figure 9. Two enter from the western side of the domain, one enters from the north, and one enters from the east. Of those entering from the west, characteristic I is representative of the interior regime, and characteristic R passes through the recirculation regime. Characteristics I and R both start in the Gulf Stream region of the interior regime, but R turns rapidly to the south and west while I continues into the interior of the basin. I passes through the Sverdrup region of the interior regime, where its trajectory appears much like the wind-driven Sverdrup circulation. In the recirculation regime, the characteristics turn rapidly to the west as they move southward. Trajectory SE enters the domain from the eastern boundary just south of the point where the zonal characteristic velocity changes sign from eastward to westward, and hence it marks the boundary between the southeastern and interior regimes.

Trajectory NE marks the northeastern regime, that region in the northeast subtropical gyre which is illuminated by characteristics which originate at the outcrop line of the first layer. Characteristics are able to enter from the north because the second layer slopes upward to the east and the Rossby wave propagation speed is to the west. If $u_c = -g\gamma_2 G_y/\gamma_1 fD$ (Rossby wave speed of zero), then the characteristics would exactly follow the outcrop, i.e., $u_c/v_c = -D_y/D_x$, and no characteristics could enter from the north. Because the Rossby wave contribution to the zonal characteristic velocity is negative, $u_c/v_c < -D_y/D_x$, and characteristics are forced to enter at the outcrop line.
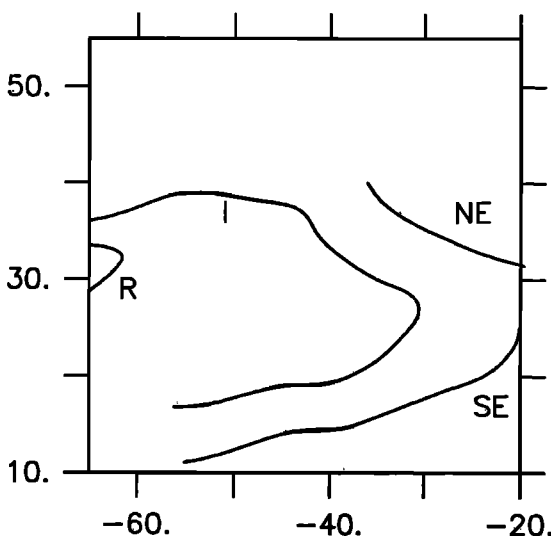

Fig. 9. Characteristic trajectories: I, interior regime; R, recirculation regime; NE, northeastern regime; SE, southeastern regime.

It is also noted that these characteristics do not recirculate through the subtropical gyre but rather extend to the east, into the near-coastal region where the present model assumptions break down. The quantitative aspects of the characteristics in this region should be interpreted with some caution because our assumption that $\eta \ll h, D$ is not very good here, but it is believed that the qualitative aspects are valid.

5. CONCLUSIONS

An idealized, two-moving-geostrophic-layer diagnostic model has been applied to the climatological hydrographic data set of *Levitus* [1982]. Estimates of the annual mean mass flux from the mixed layer into the upper thermocline (mixed layer pumping, positive upward) and subsurface heating rates were obtained on the basin scale from hydrographic data alone; no independent measures of wind stress or other surface forcings were required. In addition, the role of the nonlinear interfacial flux terms in balancing the subsurface buoyancy flux was described. Evidence is presented for the existence of separate dynamical regimes in the North Atlantic, including interior, southeastern, northeastern, and recirculation regimes.

The present analysis indicates that the mixed layer pumping is negative over most of the subtropical gyre, representing a net mass flux from the mixed layer into the upper thermocline in the annual mean. Just to the south of the Gulf Stream there is a local maximum in the negative flux which influences the propagation of characteristics there. The mixed layer pumping is of the opposite sense to the north of the Gulf Stream and in the southeastern corner of the shadow zone, driven primarily by Ekman suction in both regions. The interpretation of the mixed layer pumping throughout the domain is consistent with the annual mean Ekman pumping and the shoaling of the mean mixed layer depth by the upper layer velocity field. This result indicates that the interaction between the mixed layer and the upper thermocline flow is an important component of the surface forcing over much of the subtropical gyre.

It is found that buoyancy forcing is active over much of the upper thermocline of the North Atlantic. The patterns found here (at a depth of 200 m to 300 m) are similar to the surface density flux calculated by *Schmitt et al.* [1989]. In the mid-latitudes of the subtropical gyre, we find heating of approximately 4 W m^{-2}, driven by the nonlinear terms which are larger than, and of opposite sign to, the vertical velocity. The relative importance of the nonlinear terms was found to be a strong function of position. The nonlinearities are weaker in the beta triangle region and the shadow zone of the eastern basin and stronger in the western portion of the subtropical recirculation and in the Gulf Stream. The interior of the gyre is an indirect cell, stressing the three-dimensional aspect of the flow, while the shadow zone is described as a direct cell. The Gulf Stream is a region of strong cooling driven by the counterclockwise rotation of the velocity vector with depth and the Jacobian terms.

The quasi-linear form of the governing equations was used to define characteristic velocities and characteristic trajectories. This technique was previously used by *Luyten and Stommel* [1986] to solve for the layer depths. We make use of it here for intercomparison with that study and as an interpretive aid to better understand the propagation of information in the system. There exist interior, southeastern, north-

eastern, and recirculation regimes. The interior regime obtains its information along characteristics that enter through the northern half of the western boundary. It may be further distinguished by a Gulf Stream region, where characteristics are confined to a narrow latitude band and travel very fast, and by a broad Sverdrup recirculation region, where characteristics travel very slowly. The southeastern regime is illuminated by characteristics that enter from the southern half of the eastern boundary. The northeastern part of the basin is influenced by characteristics which originate at the outcrop of the upper layer, forced by the westward Rossby wave contribution to the zonal characteristic velocity and the nonzonal outcrop of the layer depth. Just south of the Gulf Stream the characteristics are found to turn rapidly to the west over a latitude band of 300 km. This is the recirculation regime, driven by a local maximum of the Ekman pumping.

It is demonstrated here that one can make diagnostic use of analytic theories in the analysis of historical data sets to yield relatively simple solutions that give us a direct link between theory and observations. Understanding of both the observed ocean circulation and these simple models may be advanced through this marriage of the diagnostic and analytic methods. The results found here indicate that hydrographic data sets, such as that of Levitus [1982], can support such diagnostic calculations. In addition, such analysis may lead to additional phenomena not included in the simpler representations of the ocean circulation which are necessary to yield complete analytic solutions. We are encouraged by these results to apply similar diagnostic techniques to more complex models which are not tractable through purely analytic methods. The analytic foundation of such models may be used to obtain alternative interpretations and an increased understanding of the ocean circulation that would not be attainable through traditional data analysis alone.

References

Armi, L., and H. Stommel, Four views of a portion of the North Atlantic Subtropical Gyre, *J. Phys. Oceanogr.*, *13*, 828–857, 1983.

Cushman-Roisin, B., On the role of heat flux in the Gulf Stream–Sargasso Sea subtropical gyre system. *J. Phys. Oceanogr.*, *17*, 2189–2202, 1987*a*.

Cushman-Roisin, B., Subduction, in *Dynamics of the Oceanic Surface Mixed Layer, Proceedings, 'Aha Huliko'a, Hawaiian Winter Workshop, Univ. of Hawaii at Manoa, Jan. 14–16, 1987*, Hawaii Inst. of Geophysics Special Publication, edited by P. Müller and D. Henderson, pp. 181–196, Univ. of Hawaii, Honolulu, Hawaii, 1987*b*.

Isemer, H. J., and L. Hasse, *Bunker Atlas of the North Atlantic Ocean, volume 2, Air–Sea Interactions*, Springer-Verlag, New York, 1987.

Leetmaa, A., and A. F. Bunker, Updated charts of the mean annual wind stress convergences in the Ekman layers, and Sverdrup transports in the North Atlantic, *J. Mar. Res.*, *36*, 311–322, 1978.

Levitus, S., Climatological atlas of the world ocean, *NOAA Prof. Pap. 13*, U.S. Dept. of Commerce, Washington, D.C., 173 pp., 1982.

Luyten, J. R., and H. Stommel, Gyres driven by combined wind and buoyancy flux, *J. Phys. Oceanogr.*, *16*, 1551–1560, 1986.

Luyten, J. R., J. Pedlosky, and H. Stommel, The ventilated thermocline, *J. Phys. Oceanogr.*, *13*, 292–309, 1983.

Luyten, J., H. Stommel, and C. Wunsch, A diagnostic study of the northern Atlantic subpolar gyre, *J. Phys. Oceanogr.*, *15*, 1344–1348, 1985.

Pedlosky, J., On the relative importance of ventilation and mixing of potential vorticity in mid-ocean gyres, *J. Phys. Oceanogr.*, *13*, 2121–2122, 1983.

Pedlosky, J., The buoyancy and wind-driven ventilated thermocline, *J. Phys. Oceanogr.*, *16*, 1077–1087, 1986.

Rhines, P. B., and W. R. Young, A theory of the wind-driven circulation, I, Mid-ocean gyres, *J. Mar. Res.*, *40*, Suppl., 559–596, 1982.

Schmitt, R. W., P. S. Bogden, and C. E. Dorman, Evaporation minus precipitation and density fluxes for the North Atlantic. *J. Phys. Oceanogr.*, *19*, 1208–1221, 1989.

Spall, M. A., Cooling spirals and recirculation in the Subtropical Gyre, *J. Phys. Oceanogr.*, in press, 1991.

M. A. Spall, Woods Hole Oceanographic Institution, Woods Hole, MA 02543.